GPS in Mid-life with an International Team of Doctors

Analyzing IIF-1 Satellite Performance and Backward-Compatibility

Grace Xingxin Gao, Liang Heng, Gabriel Wong, Eric Phelts,
Juan Blanch, Todd Walter, and Per Enge
Stanford University, USA

Stefan Erker, Steffen Thoelert, and Michael Meurer
DLR, Germany

ABSTRACT

With the launch of the first GPS IIF satellite, IIF-1 or SVN 62 on May 27, 2010, the U.S. GPS enters its mid-life. The IIF-1 satellite is the very first GPS satellite with an operable L5 payload. The IIF-1 L1 and L2 signals were turned on June 6, 2010, and were set "healthy" on August 27, 2010. The satellite started to transmit L5 signal on June 17, 2010.

We formed an international team of doctors. We have been continuously observing the IIF-1 transmission using a variety of facilities since the satellite was launched.

This paper shows our examination results of the IIF-1 satellite using our high gain parabolic dish antennas at Stanford USA and at Weilheim, Germany, as well as a global commercial receiver network. Our analyses of the IIF-1 satellite focus on the backward compatibility. In other words, the IIF-1 L1 and L2 signals need to be compatible with other existing satellites of older generation. We conclude that the IIF-1 L1 and L2 signals have a performance similar to other satellites in terms of range accuracy, ephemeris accuracy, signal waveform deformation, and code carrier divergence.

INTRODUCTION

The space segment of the Global Positioning System (GPS) is composed of medium earth orbit satellites of different generations. The current operational constellations contain IIA, IIR and IIR-M constellations. The next generation of constellation is the IIF system with 12 planned satellites. The IIF system is more advanced than the current constellations. It will provide twice the navigational accuracy of the existing satellites. It will also transmit more robust signals for civil aviation, and will be more resistant to interference and jamming. A chart of the broadcast civil signals by different generations of the GPS satellites is illustrated in Figure 1.

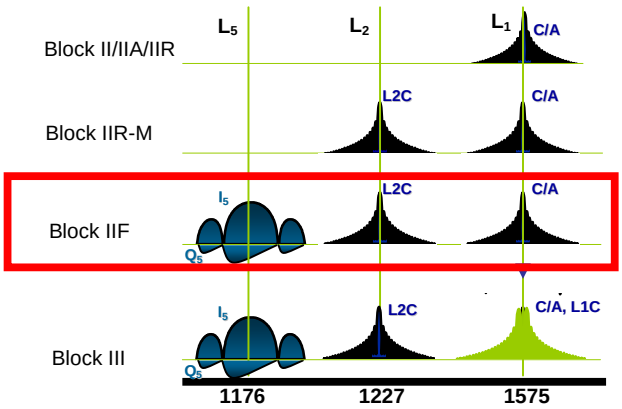

Figure 1. GPS civil signal evolution [1]

An exciting feature of the IIF-1 satellite is the L5 payload. Although a demonstration L5 payload was added to the IIR-M 20 satellite in April 2009 [2], the L5 signal transmitted by IIF-1 is intended to be a fully functioning one. Centered at 1176.45 MHz frequency in the Aeronautical Radionavigation Services band, the L5 signal has about twice the transmission power as L1 or L2C signals. [3] Compared with the L1 C/A signal, the L5 bandwidth is 10 times wider and the spreading code is 10 times longer, which yields a processing gain increase of ten times. [4]

Figure 2. The first GPS IIF satellite was launched successfully carried aboard a United Launch Alliance Delta IV rocket at 11:00 p.m. EDT May 27 from Pad 37 at Cape Canaveral Air Force Station, Florida. [5]

The very first GPS IIF Satellite out of the twelve, Space Vehicle 1 (SV-1) , or SVN 62 was launched on May 27 2010. [5] Built at Boeing's manufacturing facility at El Segundo, CA, the SV-1 satellite has successfully completed ground tests in September 2009 [6], and was shipped to Cape Canaveral Air Force Station in Florida in February 2010 [7]. Based on our observations, the signals in L1 and L2 frequency bands of the IIF-1 satellite were turned on June 6, 2010. The L5 signal was then turned on June 17, 2010. By July 28, 2010, the satellite was settled with its final transmission scheme listed in Table 1 below. The L1 and L2 signals of IIF-1 were set "healthy" on August 27th. [8]

Frequency Band	Transmitted Signals
L1	C/A, P(Y), and M codes
L2	L2: L2C, P(Y), and M codes
L5	data & pilot

Table 1. IIF-1 transmitted civil signals in different frequency bands

This paper presents the first observation and analysis of the GPS IIF SV-1 satellite signals. We formed an international team of "doctors" to examine the new IIF satellite. The paper focuses on the backward compatibility of the IIF-1 satellite. Since the L1 and L2 signals were set healthy, we would like to verify that the first satellite of the new Block IIF generation is compatible with the older generations of satellites, such as Block II/IIA/IIR and IIR-M.

The paper is organized as follows. We will first introduce our world-wide signal observation facilities in two categories – high gain dish antennas and commercial receivers. The main body of the paper will be focused on backward compatibility, in the following aspects: range accuracy, ephemeris accuracy, signal powers, signal waveform deformation, and code carrier coherence. Finally, we will conclude the paper.

WORLD-WIDE SIGNAL OBSERVATION FACILITIES

To verify the signal quality and performance of this new GPS generation the signals of IIF SVN-62 are captured and analyzed continuously from the beginning by independently using a variety of facilities world-wide. The facilities are grouped into two categories, high gain dish antennas with vector signal analyzers, and commercial receivers with patch antennas.

A. High Gain Antennas

The dish antennas have the advantage of high antenna gain, and thus enable close observation of the IIF-1 signals at chip and waveform levels.

We used three high gain dish antennas for our observation - the 45-meter Stanford SRI dish, the 30-meter DLR dish, and the 1.8-meter Stanford dish, as shown in Figures 3 -5 respectively. The Stanford SRI dish is the biggest and has the highest gain. However, it requires scheduling and is only available for limited times. The Stanford 1.8 meter is smaller with less antenna gain, but it is easy to access. The DLR dish provides data from the other side of the earth, which is complementary to the Stanford dish data. All the three dishes are connected with bandpass filters, low noise amplifiers, and vector signal analyzers. Papers [9, 10] contain details of these dish antennas.

Figure 3. Stanford SRI 45-meter dish at Stanford CA, USA

Figure 4. DLR 30-meter dish at Weilheim, Germany

Figure 5. Stanford 1.8 meter dish at Stanford CA, USA

B. Commercial Receivers

Although the dish antennas provide data with high signal-to-noise ratio, due to the data rate of the raw data as high as 70 Mbps, data length is only on the order of minutes or even seconds.

Commercial receivers record processed measurement data, such as pseudo-range measurements and ephemeris data. The data rate is normally as low as 1 to 50 Hz. Due to the low data rate, we use commercial receivers to log data for days, weeks and months for continuous observation.

We set up a commercial multi-frequency GNSS patch antenna on the roof of the GPS lab at Stanford, CA. We use a splitter to split the incoming signal into two: one connecting to a commercial multi-frequency multi-constellation receiver, the other connecting to a commercial L1 band only receiver, as illustrated in Figure 6.

Figure 6. Commercial receivers setup in the GPS lab at Stanford, CA. The incoming signal received by a commercial patch antenna is split into two paths, one connecting to a commercial multi-band multi-constellation GNSS receiver, the other connecting to a GPS L1 only receiver.

We also gather data from the International GNSS Service (IGS) network [11]. The IGS network has over 350 receivers all over the world as shown in Figure 7. They output both the range measurements and the ephemeris information in RINEX format.

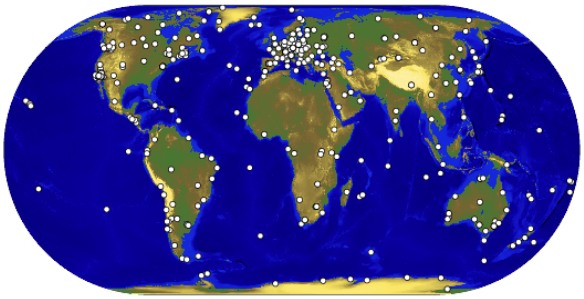

Figure 7. 364 IGS stations all over the world

BACKWARD COMPATIBILITY

The IIF-1 satellite is the first satellite of the new Block IIF generation. In addition to the new L5 signal, the L1 and L2 signals are required to be interoperable with existing satellites. In other words, the IIF-1 satellite is required to have backward compatibility. In this section, we conduct our analysis in the following aspects: range accuracy, ephemeris accuracy, signal power, signal deformation, and code carrier coherence.

A. Ephemeris Accuracy

Ephemeris errors are calculated by the difference between broadcast and precise ephemerides. The precise ephemerides are obtained from The National Geospatial Intelligence Agency (NGA) network. NGA network has 12 stations all over the world. The stations output the post-processed truth ephemerides including satellite position and the clock, plus the change rate of position and clock every 15 minutes. [12] The broadcast ephemerides are obtained from a commercial receiver set up in the GPS lab at Stanford, CA. The broadcast ephemerides are projected to the same time stamps as the NGA truth to make the comparison.

The satellite position errors, i.e. along-track, and cross track errors are shown in Figure 8. The along-track and cross-track errors are within +/- 3 meters. The radial errors are smaller, only within +/- 0.5 meter. clock errors are calculated as well, which are within 0.7 meter.

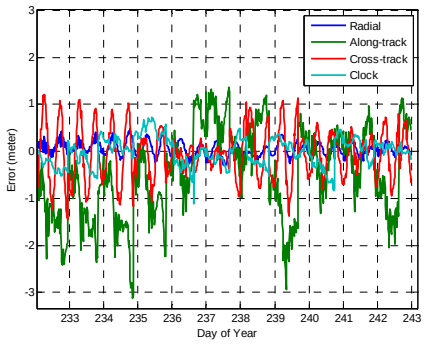

Figure 8. Ephemeris errors, including radial, along-track, cross-track, and clock errors are bounded within +/- 3 meters, which are within the specification.

B. Range Accuracy

In order to obtain the range accuracy, we projected the ephemeris and clock errors from the previous section onto a grid of user spaced 1 degree apart. We calculate the signal-in-space range errors projected to the line between the IIF-1 satellite and the receiver grid points.

Figure 9 plots the worst case and global average of the projected satellite signal-in-space (SIS) errors over ten days since the satellite was set healthy. The average SIS errors are within [-1, 1] meter; while the worst-case SIS errors are bounded within [-1.5, 1.5] meters. We also checked the range accuracy rate and range accuracy acceleration. They are all within the specifications. [14]

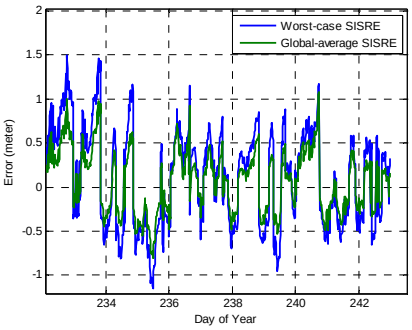

Figure 9. Worst case and global average of the projected satellite signal-in-space errors over ten days since the satellite was set healthy. The range accuracy is within specification.

C. Signal Power

We also investigated on the signal power. Figure 10 shows the signal-to-noise ratio (SNR) of IIF-1 satellite and those of other existing GPS satellites versus elevation angle on June 19, 2010. The L1 data are obtained from from 'wsrt' site at Westerbork Synthesis, Netherlands of the IGS network. The receiver type is AOA SNR-12 ACT.

It is obvious that the IIF-1 L1 signal power is greater than other satellites by about 3 dB, especially at high elevation. We plot the satellite signal to noise ratio again on September 15, 2010. As shown in Figure 11, the SNR of the IIF-1 L1 signal is still higher than its peers, although reduced by about 1 dB compared to an earlier data of June 19, 2010.

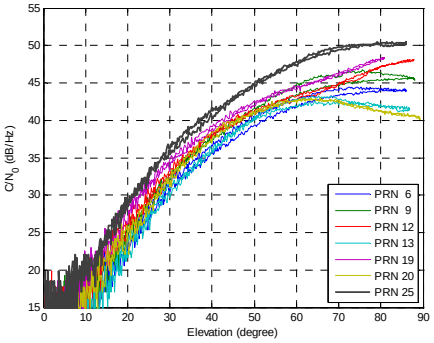

Figure 10. IIF-1 L1 signal has higher power than other GPS satellites. Data collected on June 19, 2010.

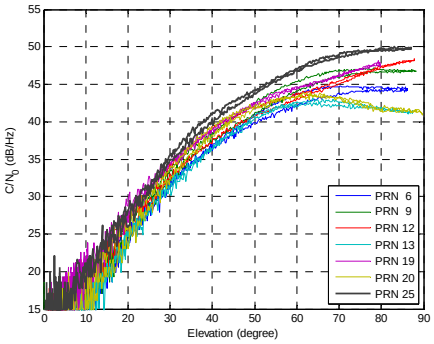

Figure 11. IIF-1 L1 signal still has higher power than other GPS satellites, although the gap has been reduced. Data collected on September 15, 2010.

D. Signal Deformation

Assuming no internal reflections or elevation angle dependencies, there are two types of signal deformations: analog and digital.

Analog deformations result from filter limitations in either the signal transmission path or the receiver hardware. Analog deformation creates oscillations in the signal waveform that cause the correlation peak to become asymmetric.

Digital distortions occur when timing of the individual chip transitions of the transmitted codes are either in advance or delayed from the ideal falling or rising edges of a code chip. Digital distortion flattens the correlation peak.

To characterize either type of distortion requires high-gain, high-resolution measurements of the transmitted signals.

The following sections compare both types of nominal deformations for IIF-1 to those measured for the legacy constellation of satellites. The analyses are based on data from our high-gain dish antennas described in the previous section.

Figure 12 shows the L1 signal waveform. The ringing in the chip waveform rather than an ideal rectangular shape is due to the analog deformation of the signal.

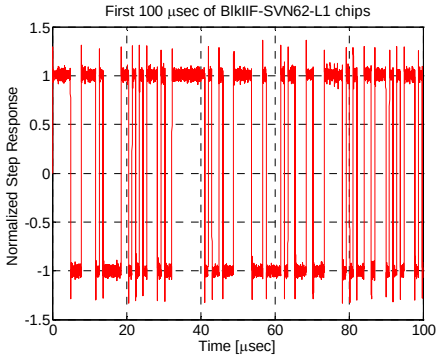

Figure 12. IIF-1 L1 signal waveform. The ringing in the chip waveform rather than an ideal rectangular shape is due to the analog deformation of the signal.

Next, we compare the analog deformation of the IIF-1 L1 signal with other GPS satellites. Figure 13 plots the C/A code step-responses of IIF-1 L1 signal together with those of other GPS L1 signals. It is seen that all the responses for all the satellites are fairly similar. Each has an overshoot ranging from about 120% of the steady-stare amplitude, and the overshoot for IIF-1 lies approximately in the middle of this range. The step response for IIF-1 does, however, seem to be more damped. Its settling time appears significantly smaller than for the other responses.

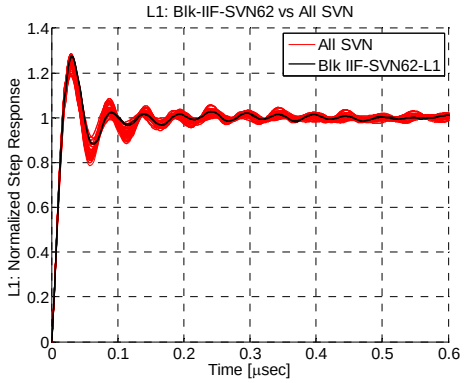

Figure 13. Comparison of the step responses of the IIF-1 L1 C/A codes with 17 other GPS satellites. (The response of SVN62 is depicted by the heavy black trace.) IIF-1 L1 analog signal deformation similar to that of past L1 satellites.

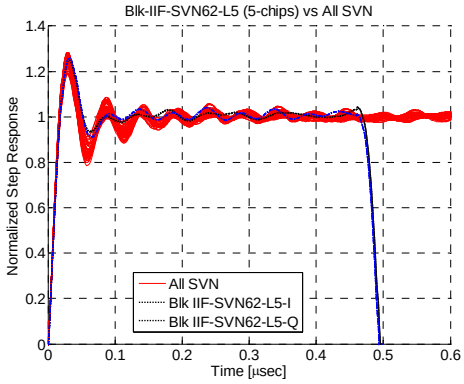

Figure 14. Comparison of the step responses of IIF-1 L5 signal with other satellites. IIF-1 L5 analog signal deformation is similar to that of past L1-satellites.

Figure 14 compares the step responses of IIF-1 L5 chip waveform with the L1 C/A waveform of other GPS satellites. Since the L5 signal has 10 times the bandwidth of the C/A signal, the L5 chip width is only 1/10 of the C/A chip width. In order to better compare the effects of the filter after transition, segments of the L5 code that had five positive chips in row were selected for display in the figure. Thus, what is shown is five times longer than a single L5 chip width. As expected, the L5 I and Q signals agree quite closely with each other. Ideally, these would be identical since all the signals pass through the same filtering components on the satellite. However, some small differences can be seen. Measurement error may account for some of the differences observed. The L1 C/A signal shape is quite similar to the L5 response, which indicates similar filter designs in the two different frequency paths.

Compared to the L5 demo signal of GPS IIR-M SVN49 that only transmitted a dataless Q-component signal, the operational IIF L5 signal consists of an I and Q component. The scatter plot of the I and Q components is plotted in Figure 15. Ideally, a symmetric square with two straight diagonals should be observed. However, the transition from I-Q state [1, 1] to [-1, -1] is distorted. The reason is the digital distortion. To be specific, when transitioning from [1, 1] to [-1, -1], the transition in I channel is slower or delayed compared to the Q channel, causing the diagonal shown in Figure 15 bent downwards. With the chip rate of 10.23 MHz, the L5 signal is supposed to have a chip width of 98 nsec. Our observation shows that in-phase positive chips are on average 9 nsec longer than the quadrature positive chips. In-phase negative chips are on average 9 nsec shorter than the quadrature negative chips.

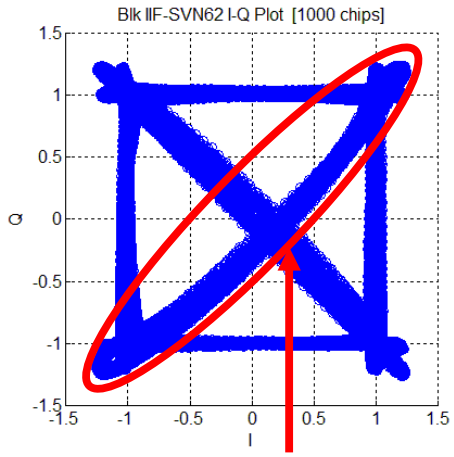

Figure 15. The I-Q plot of IIF-1 L5 signal. Digital distortion is observed.

E. Code Carrier Divergence

In early 2009, the navigation community got its first look at an L5 signal transmitted from a GPS satellite—SVN49. The Block IIRM satellite had been retrofitted with an L5 transponder to temporarily reserve spectrum for the upcoming Block IIF satellites. Unfortunately, that retrofit had the unintentional side-effect of code carrier divergence on L1 signal.

The details of this reflected signal have been studied and documented. [13] The transmitted signal is internally distorted by multipath. Worse yet, this distortion created errors that vary as a function of user receiver implementation and elevation angle.

The following question naturally rises: "Does an elevation dependent bias also exist for IIF-1?" To answer this question, we processed the data from network to compare the elevation angle dependence of the two satellites. The same IGS site was used for both SVN 49 and SVN 62 in our study so that the receiver errors are comparable for each. The IGS site was selected based on the following requirements:

1. The receiver outputs measurements for both SVN 49 and SVN 62 satellites. As both satellites are set 'unhealthy' at this moment, many IGS sites do not output their measurements. All 300+ receivers in the IGS network were screened; only 69 of them provide data for both satellites as of Day 170, Year 2010.
2. The receiver observes both SVN 49 and SVN 62 at high elevation angles. As we evaluate the elevation dependency, we want the full (or near-full) span of the elevation. Figure 1 shows the ground tracks of the two satellites. We favored the receivers located in the vicinity of the cross point marked by a red circle.
3. The receiver noise is low. The two nearest receivers to the ground track cross point are 'brus' (Brussels, Belgium) and 'wsrt' (Westerbork, the Netherlands). We choose 'wsrt— a TurboRogue AOA SNR-12 receiver— for investigation. Although it is the second-nearest site, its receiver noise and multipath is lower than 'brus' based on our study. The longitude, latitude, and height of the site are +4.3592 degrees° (Longitude), +50.7978° (Latitude) and 149.7 m (above geoid) respectively.

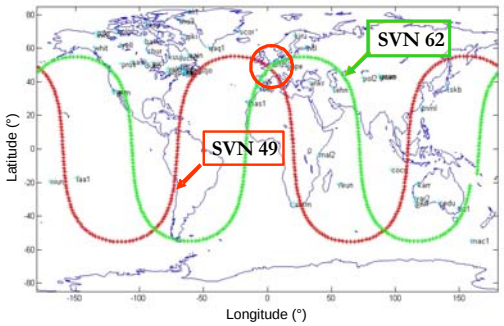

Figure 16. Ground tracks of SVN 49 and SVN 62. The receivers shown on this map are the 69 out of 300+ IGS sites that output both SVN 49 and SVN 62 measurements as of Day 170, Year 2010.

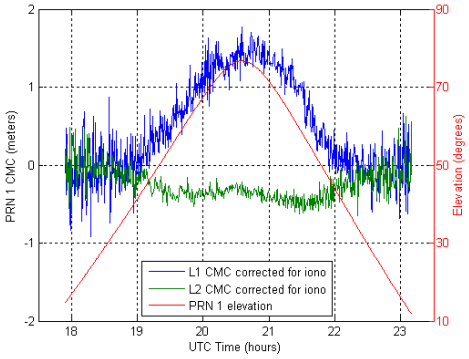

Figure 17. SVN 49 code-minus-carrier measurements after applying a dual-frequency ionosphere correction. The clock, orbit, troposphere, and ionosphere errors are all eliminated. An obvious positive elevation-dependent bias exists in the L1 C/A measurements. A slight negative elevation-dependent bias is seen in the L2 measurements.

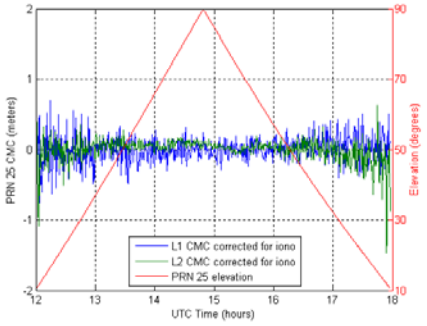

Figure 18. SVN 62 code-minus-carrier measurements after applying a dual-frequency ionosphere correction. The clock, orbit, troposphere, and ionosphere errors are all eliminated. No apparent elevation-dependent bias exists in either L1 or L2 measurements.

We use the following equations to compute code carrier divergence for L1 and L2 signals.

For L1 signal,
$L1_{PR} - L1_{CR} + 2 * (L2_{CR} - L1_{CR}) / (g-1)$,
where
$L1_{PR}$ is L1 pseudo range measurements,
$L1_{CR}$ is L1 carrier phase measurements,
$L2_{PR}$ is L2 pseudo range measurements,
$L2_{CR}$ is L2 carrier phase measurements,
$g = (1.57542/1.2276)^2$.

For L2 signal,

$L2_{PR} - L2_{CR} + 2 * g*(L2_{CR} - L1_{CR}) / (g-1)$.

The elevation-angle effect was readily apparent on the measurements of SVN 49 received on June 19, 2010 and presented in Figure 17. (This bias was further verified by checking the data from other IGS sites and NSTB sites.) It shows the code/carrier difference for a single frequency after applying dual-frequency carrier-based ionosphere error corrections. Clock, orbit, troposphere, and ionosphere errors are all removed. The figure indicates that the SVN 49 anomaly is primarily in the L1 band; the code-minus-carrier (CMC) with ionosphere correction for PRN 1 has a bias highly correlated with the satellite elevation. The bias has a relative shift of 1.5 meters from a low elevation of 15° to a high elevation of 77°. The L2 CMC curve is flatter, although there appears to be a bias of about 0.4m in the opposite direction.

Figure 18 shows a similar plot for the L1 signal on SVN 62. The plot reveals there is no noticeable dependence on elevation angle from a low elevation of 10° to a high elevation of 89°.

CONCLUSION

An international team of doctors from Stanford and DLR examined the first GPS IIF satellite as GPS enters its mid-life. We focus on backward compatibility of the satellite. Specifically, we conducted analyses in terms of range accuracy, ephemeris accuracy, signal power, signal waveform analog and digital deformation, and code carrier divergence for L1 and L2 signals. We conclude that the IIF L1 and L2 signals have a performance similar to those of other existing satellites. In other words, the IIF-1 satellite is backward compatible with older generation satellites. For IIF-1 L5 signal, we have observed digital distortion of the signal waveform. As the IIF-1 L5 signal is still in its testing mode, such a distortion is continuously monitored.

ACKNOWLEDGMENTS

The authors gratefully acknowledge the support of the Federal Aviation Administration under Cooperative Agreement 08-G-007. This paper contains the personal comments and beliefs of the authors, and does not necessarily represent the opinion of any other person or organization.

REFERENCES

[1]. Lt Col Wayne Bell, GPS Program Update, Civil Global Positioning System Service Interface Committee Meeting, September 2005.

[2]. Grace Xingxin Gao, Liang Heng, David De Lorenzo, Sherman Lo, Dennis Akos, Alan Chen, Todd Walter, Per Enge and Bradford Parkinson, Modernization Milestone: Observing the First GPS Satellite with an L5 Payload, Inside GNSS Magazine, May-June 2009.

[3] Spilker, J. J., Van Dierendonck, A. J., Proposed New Civil GPS Signal at 1176.45 MHz, Proceedings of the 12th International Technical Meeting of the Satellite Division of the Institute of Navigation ION GPS-1999, September 1999.

[4]. R. Eric Phelts, Grace Xingxin Gao, Gabriel Wong, Liang Heng, Todd Walter, Per Enge, Stefan Erker, Steffen Thoelert, and Michael Meurer, Aviation Grade, New GPS Signals Chips Off the Block IIF, Inside GNSS Magazine, July-August 2010.

[5]. Block IIF Successfully Launched from Cape Canaveral, GPS World Magazine, May 2010.

[6]. Boeing Completes Ground Tests for First GPS IIF Satellite Launch, GPS World Magazine, September 2010.

[7]. Glen Gibbons , Behind the GPS IIF Launch: A Long and Winding Road, Inside GNSS Magazine, June 2010.

[8]. Richard B. Langley, First GPS Block IIF Satellite Set Healthy, GPS World Magazine, August 2010.

[9]. Sherman Lo, Alan Chen, Per Enge, Grace Xingxin Gao, Dennis Akos, Jean-Luc Issler, Lionel Ries, Thomas Grelier and Joel Dantepal, GNSS Album: Images and Spectral Signatures of the New GNSS Signals, Inside GNSS Magazine, May-June 2006.

[10]. Steffen Thoelert, Steffen Erker, Michael Meurer, Liang Heng, Eric Phelts, Grace Xingxin Gao, Gabriel Wong, Todd Walter, and Per Enge, On the Air, New Signals from the First GPS IIF Satellite, Inside GNSS Magazine, July-August 2010.

[11]. International GNSS Service (IGS) network, http://igscb.jpl.nasa.gov/

[12]. National Geospatial Intelligence (NGA) network, http://earth-info.nga.mil/GandG/sathtml/ephemeris.html

[13]. Grace Xingxin Gao, Liang Heng, David De Lorenzo, Sherman Lo, Dennis Akos, Alan Chen, Todd Walter, Per Enge and Bradford Parkinson, Modernization Milestone: Observing the First GPS Satellite with an L5 Payload, Inside GNSS Magazine, May-June 2009.

[14]. GPS SPS Signal Specification, 2nd Edition, June 1995. Downloadable at http://www.navcen.uscg.gov/pubs/gps/sigspec/default.htm